Self-organized Criticality and Phase Problem in Magnetoacoustic Emission Burst in Ferromagnets

M. Namkung, J. P. Fulton† and B. Wincheski†

NASA Langley Research Center, Hampton, VA 23681
†Analytical Services and Materials, Inc., 107 Research Dr., Hampton, VA 23666

ABSTRACT

Two types of ferromagnets, pure iron and steel with varying geometry and microstructural properties, were prepared for the present study of magnetoacoustic emission (MAE). The purpose was to separate the effects of structural property variations from changes caused by differences in the sample geometry. The position and shape of the leading MAE sub-burst and its variation among the samples are explained by magnetic anisotropy and the results of numerical simulations which utilized the concept of self-organized criticality (SOC). The amplitude and duration of the second sub-burst, which previously was thought to occur as a result of a complicated interaction between non-180^{o} domain walls and lattice defects, can easily be explained by the results of our simulation.

I. INTRODUCTION

All of the previous MAE tests of various types of steel were analyzed based upon the magnetic properties of iron. Reasonable interpretations of test results were obtained, especially for the uniaxial stress dependence of the MAE spectral characteristics [1,2,3]. There exists, however, several elements related to certain basic properties of MAE that are unexplained. First, the presence of two sub-bursts during a sweep over one half cycle of the hysteresis loop. Furthermore, under normal conditions, i.e., without having a significant stress or a pronounced rearrangement of defect structures, the leading sub-burst is usually sharp and narrow. At the same time, the trailing sub-burst is, in general, seen to be smooth and its duration is much longer than that of the leading sub-peak. Finally, the position of the leading sub-burst usually occurs long before the major change in the net magnetic flux. Some qualitative explanations can be found for these MAE characteristics, but they are no more than phenomenological illustrations, as will be discussed later in this paper. Consequently, a more detailed study was necessary to gain a deeper insight into the physical processes involved in MAE.

The present study includes both experimental and numerical work. Two types of ferromagnets, high purity polycrystalline iron and low carbon steel, of three different thicknesses were used. The iron samples were apparently rolled to differing degrees to form thin sheets of various thicknesses with a diverse miscrostructure, i.e., the elongation of grains varied. This was especially pronounced in the thinnest sample. In order to distinguish the effects of such microstructural variations from the sample thickness dependence, if there is any, a set of samples were made from a single low carbon steel block [See Ref. 4 for the properties of this steel]. In Section II we briefly describe the samples used along with the experimental procedure. The MAE test results are presented in Section III along with a description of the characteristic elements.

The numerical simulation is based on the relatively new concept of self-organized criticality. The model is constructed on the assumption that there are two separate distributions of domain wall motion-resisting potential barriers. The results of the numerical simulations are surprisingly consistent with that of the experiment, despite the model's simplifications which lack of a direct link to physical principles. The results strongly suggest that the unexplained characteristics of the MAE spectra may simply be due to the self-organizing process of the physical system. The details of the simulation are presented in Section IV which is followed by a summary.

II. EXPERIMENTS

The first set of test samples consisted of three pure iron (99.999%) plates with a two dimensional area of 6 x 1.5 cm^2. These samples were available in three different thicknesses: 0.5, 1.25 and 2.5 mm. The degree of rolling varied among samples of different thicknesses and grain elongation was most severe in the thinnest sample, as was found by studying optical micrographs. Hence, another set of samples having the same geometry as the pure iron samples was prepared from a single block of low carbon steel. The metallurgical information and manufacturing processes can be found in Ref. 4. Throughout the experiments, the peak amplitude of the applied magnetic field at the surface was kept at 72 Oe and the frequency of the AC magnetic field was fixed at 30 Hz. The resultant MAE spectrum was obtained by averaging over 50 bursts. The details of the MAE experiment can be found elsewhere [1,2,3,4].

III. EXPERIMENTAL RESULTS AND DISCUSSION

Fig. 1 shows the oscilloscope trace of the induc-

tion pickup coil output (upper trace) and the MAE burst (lower trace) both averaged over 50 frames for the 0.5 mm thick pure iron sample. The point where the pickup coil output has a maximum output corresponds to the maximum rate of change in the net magnetic induction due to the motion of magnetic domains. The position of the peak of the leading sub-burst in Fig. 1 is seen to occur much earlier than the point where the domain wall motion is most active.

Fig. 2 shows the results obtained with the 0.5 mm thick steel sample. The position of the peak of the leading sub-burst in this figure is not as advanced as that shown Fig.1, but is noticeably earlier than the peak of the pickup coil output. In both figures one can see a second sub-burst along with a third sub-burst which occurs long after the change in the magnetic state of the sample has ended. Recent results obtained with the same samples at 0.7 Hz also showed a third sub-burst of the same nature [5]. Considering that the test results obtained with bulk samples made from

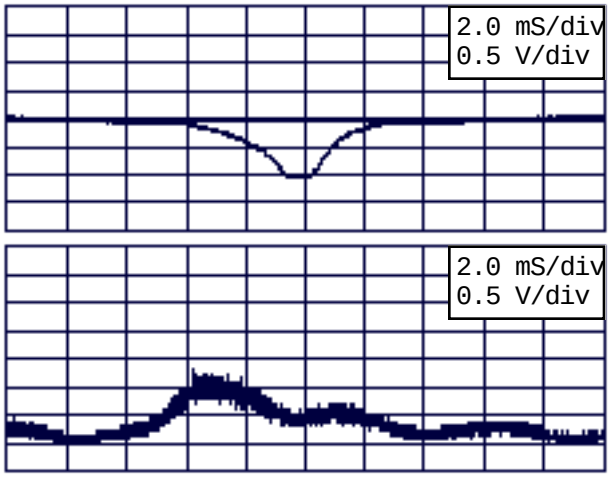

Fig. 1. Results obtained with 0.5 mm thick pure iron sample at 30 Hz.

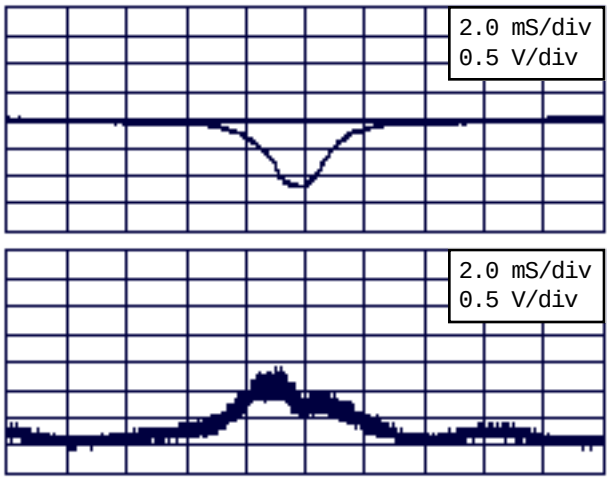

Fig. 2. Result obtained with 0.5 mm thick steel sample at 30 Hz.

the same material during the past several years never showed such an additional peak, it may be that the thinness of these samples is responsible for the occurrence of the third sub-burst. However, at the present time a more detailed explanation of this phenomena is not possible. Hence, we will focus our attention on the first and second sub-burst only.

The early appearance of the leading sub-burst was explained recently based on the local critical field at which a domain of reverse magnetization is nucleated. For pure iron these domains are formed in the vicinity of nonmagnetic inclusions, and the calculation shows that if the radius of the inclusion larger than 10^{-5}cm, the critical field strength is larger than 10 Oe in the direction of net magnetization [6]. This means that a considerable level of domain wall motion occurs before the magnetic state reaches remanence while being reduced from saturation.

The reduced MAE activity in the region of the highest pickup coil output as shown in both Fig. 1 and 2 has been observed to be a universal characteristic. This apparently is inconsistent with the basic assumption, i.e., MAE is produced by the rearrangement of the local lattice strain field due to domain wall motion and, hence, the MAE activity is enhanced as the rate of domain wall motion becomes higher. The assumption itself should be correct if the rate of change in the applied magnetic field is extremely slow.

Under the present experimental conditions, however, the basic mechanism for the change in the net magnetization is roughly due to the motion of macroscopic 180^{o} domain walls which oscillate back-and-forth, while dragging 90^{o} domain walls [7]. The motion of the 180^{o} domain walls is resisted mainly by two factors: the eddy currents generated by the change in the net magnetic flux and the delay in 90^{o} domain wall motion due to its low mobility. Both of these factors are assumed to contribute to the delayed MAE activity of the trailing sub-burst but further details are unknown at the present time.

Fig. 3 and 4 show the results obtained with 1.25 mm thick pure iron and steel samples, respectively. The difference in the positions of the leading sub-bursts in the pure iron and steel samples of these figures are seen to be much smaller than that between Fig. 1 and 2. The 0.5 mm thick pure iron sample was apparently rolled to a more severe degree of grain elongation which is assumed to be the easy magnetization direction.

During the experiments, the external field was applied along this direction of easy magnetization. This brings up an interesting point. With the iron being pure, the density of the nucleation centers for reverse magnetization domains will be low and the average local critical field for such domain creation will be smaller than that of steel. One the other hand, the higher density of impurities and defects in steel tend to pin down the 90^{o} domain wall motion. Under normal circumstances, the position of the leading sub-burst in iron and steel are almost the same due to a compromise between these two competing effects. Such

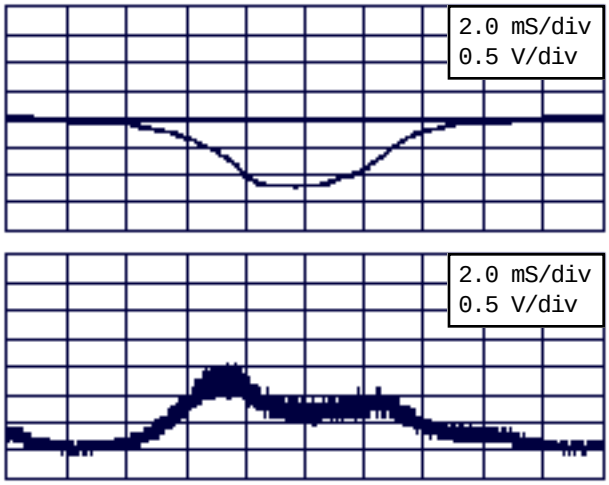

Fig. 3. Results obtained with 1.25 mm thick pure iron sample at 30 Hz.

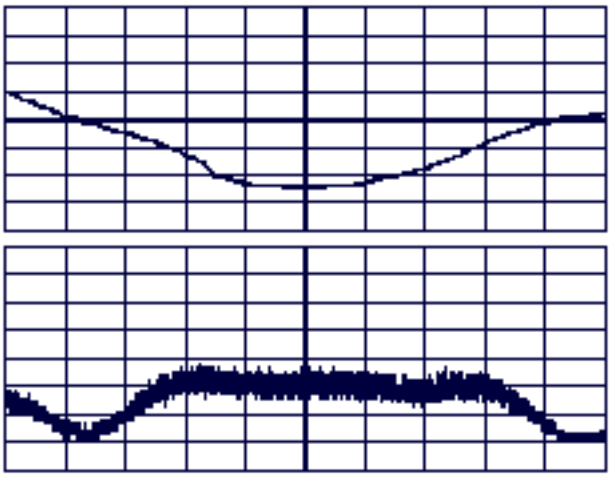

Fig. 5. Results obtained with 2.5 mm thick pure iron sample at 30 Hz.

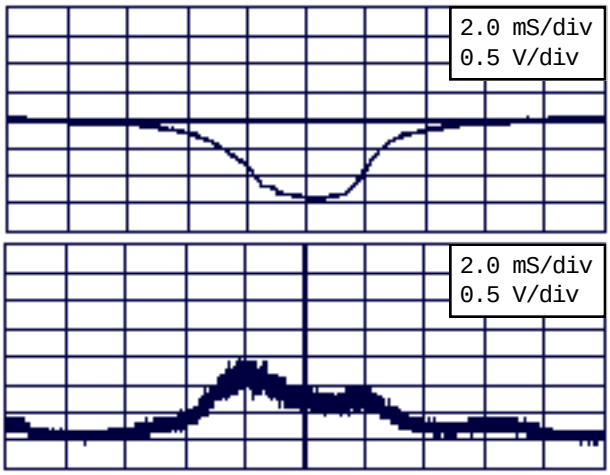

Fig. 4. Results obtained with 1.25 mm thick steel sample at 30 Hz.

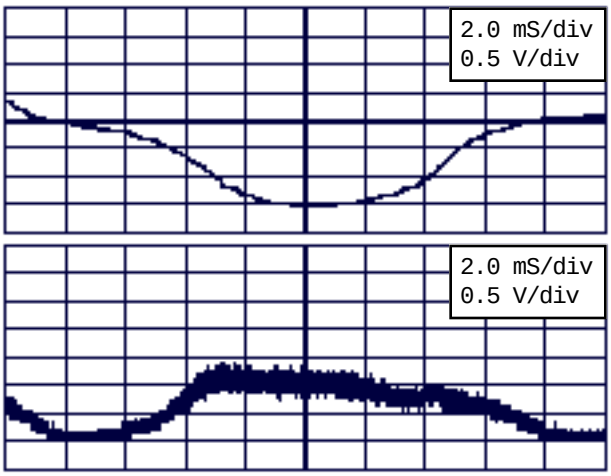

Fig. 6. Results obtained with 2.5 mm thick steel sample at 30 Hz.

a balance is disturbed when certain structural changes are introduced as in the 0.5 mm thick pure iron sample.

Fig. 5 and 6 show the results obtained with 2.5 mm. thick samples of iron and steel, respectively. Except for the slight trailing slope in the burst of Fig. 6, the overall pattern in these figures are quite similar. They both show a broad MAE peak which is confined to the range of pickup coil output and which is very different from the results of the thinner samples in Fig. 1 to Fig. 4. These results clearly indicate that there is more travel distance available for the macroscopic 180^{o} domain walls in the thicker samples and the 90^{o} domain walls are continuously pulled after being created at the domains of reverse magnetization.

IV. NUMERICAL SIMULATION INCORPORATING SELF-ORGANIZED CRITICALITY

We divide a ferromagnetic sample into discretized cells where each cell is assumed to be magnetized in accordance with the easy axes of magnetization. During their lifetime, i.e., between $|B|_{max}$ and $-|B|_{max}$ each domain will face two major potential barriers resisting their motion. The distribution of the number of cells as a function of the potential barrier height is assumed to be gaussian with a given mean and standard deviation that are entered as parameters in the model. The first barrier corresponds to the critical field necessary for the nucleation of the domains of reverse magnetization and their subsequent local expansion to reach the pinning sites. The second corresponds to the critical field necessary to cause irreversible motion over the pinning sites. The critical field strength associated with each cell was assigned randomly to the individual cells (each cell was assigned a critical field strength only once during the entire period).

The model uses is discretized in time and a sinusoidal field is applied to the array of cells. Currently, the model assumes that the field is sensed by all the cells uniformly and simultaneously, but this can be changed to account for variations caused by eddy currents and nonuniform

magnetization resulting from thickness variations. The model increments in time and the magnetization in each cell is reversed as the magnitude of the applied field reaches the given critical field strength. The magnitude of the burst at time t is simply the sum of the number of regions that moved during the time step Δt.

Introduced by Bak et. al, the concept of self-organized criticality (SOC) provides a consistent explanation of 1/f noise and fractal characteristics in dynamical systems [8]. Once perturbed, in this process, the local fluctuation of a certain physical state in a cell propagates throughout the system by generating fluctuations in the neighboring cells which causes an avalanche through a domino effect. Through the avalanche the system organizes itself to reach another barely stable state.

A simple modification to the modeling scheme was necessary to add the effects of SOC. That is, if the applied field strength reaches the critical field strength for a particular cell, the magnetization direction in the cell reverses. This reversal causes a certain amount of influence to the physical state of the nearest neighbor cells. We chose this influence to be a modification to the preassigned critical field strength with the amount of modification as an adjustable parameter. A more detailed explanation of the model can be found in Ref. 9.

Fig 7. shows the modeling results which are close to that observed for the thin samples (0.5 and 1.25 mm thick samples of iron or steel) which were obtained by broadening the first distribution to match the shape of the first sub-burst. The results of Fig. 7 can be compared with those previously obtained to match the typical test results of bulk steel samples. These results of Fig. 8 used a narrower distribution of the critical field necessary to form the domains of reverse magnetization.

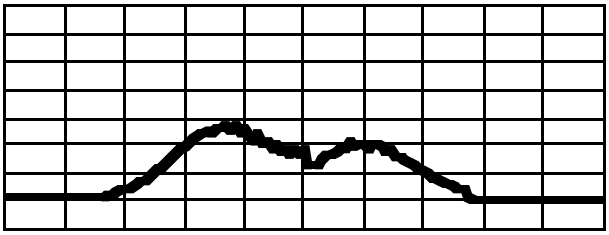

Fig. 7. Modeling results simulating the MAE burst observed in the thin samples of Fig. 1 to 4.

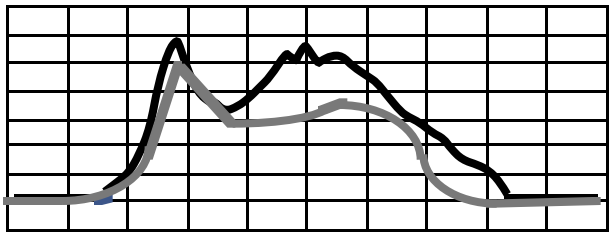

Fig. 8. Modeling (black) and experimental (gray) results for a bulk sample (from reference 9).

One can easily predict that the beginning of the self-organizing process depends on the width and the location of the distribution of the critical field strength of reverse domain nucleation. These, of course, are the major elements determining the phase and shape of the leading sub-burst of MAE.

VI. SUMMARY

The major accomplishments of the present study are: first, we provided more evidence for the role of the local critical field for the nucleation of reverse magnetization domain which causes the early appearance of the leading sub-burst and, second, from the results of the 2.5 mm samples, the confirmation of the macroscopic 180^{o} domain walls that oscillate back-and-forth during the magnetization process. It was also demonstrated that we can match the modeling results to that of experiments by changing certain parameters in the simulation. This clearly means that one can gain deeper insight in the complicated process of MAE generation and more easily identify the major physical mechanisms involved in each stage.

VII. REFERENCES

1. M. Namkung, R. DeNale and R. G. Todhunter, in *Review of Progress in QNDE*, edited by D. O. Thompson and D. E. Chimenti, Vol. 10B, 2007 (1990).
2. M. Namkung, R. DeNale, P. W. Kushnick, J. L. Grainger and R. G. Todhunter, *Proc. IEEE Ultrasonic Symposium*, Vol. 2, 1167 (1989).
3. M. Namkung, D. Utrata and R. Denale, *Proc. IEEE Ultrasonics Symp.*, Vol. 2, 983 (1990).
4. S. G. Allison, W. T. Yost, J. H. Cantrell and D. F. Hassen, in *Review of Progress in QNDE*, edited by D. O. Thompson and D. E. Chimenti, Vol. 7B, 1463 (1988).
5. M. Namkung, B. Wincheski, J. P. Fulton and R. G. Todhunter, Submitted to *Review of Progress in QNDE* (1993).
6. J. B. Goodenough, *Phys. Rev.* 95, 917 (1954).
7. S. Chikazumi, Physics of Magnetism, (John Wiley & Sons, 1964).
8. P. Bak, C. Tang and K. Weisenfeld, *Phys. Rev. Lett.* 59, 381 (1987).
9. J. P. Fulton, B. Wincheski, and M. Namkung, Submitted to *Review of Progress in QNDE* (1993).